# Mechanistic Study on the Reaction of a Radical SAM Dehydrogenase BtrN by Electron Paramagnetic Resonance Spectroscopy[†]

Kenichi Yokoyama,[‡] Daijiro Ohmori,[§] Fumitaka Kudo,[‡] and Tadashi Eguchi*[,‖]

*Department of Chemistry and Department of Chemistry and Materials Science, Tokyo Institute of Technology, O-okayama, Meguro-ku, Tokyo 152-8551, Japan, and Department of Chemistry, Juntendo University, Inba, Chiba 270-1695, Japan*

*Received March 25, 2008; Revised Manuscript Received June 29, 2008*

ABSTRACT: BtrN is a radical SAM (*S*-adenosyl-L-methionine) enzyme that catalyzes the oxidation of 2-deoxy-*scyllo*-inosamine (DOIA) into 3-amino-2,3-dideoxy-*scyllo*-inosose (amino-DOI) during the biosynthesis of 2-deoxystreptamine (DOS) in the butirosin producer *Bacillus circulans*. Recently, we have shown that BtrN catalyzes the transfer of a hydrogen atom at C-3 of DOIA to 5′-deoxyadenosine, and thus, the reaction was proposed to proceed through the hydrogen atom abstraction by the 5′-deoxyadenosyl radical. In this work, the BtrN reaction was analyzed by EPR spectroscopy. A sharp double triplet EPR signal was observed when the EPR spectrum of the enzyme reaction mixture was recorded at 50 K. The spin coupling with protons partially disappeared by reaction with [2,2-$^2H_2$]DOIA, which unambiguously proved the observed signal to be a radical on C-3 of DOIA. On the other hand, the EPR spectrum of the [4Fe-4S] cluster of BtrN during the reaction showed a complex signal due to the presence of several species. Comparison of signals derived from a [4Fe-4S] center of BtrN incubated with various combinations of products (5′-deoxyadenosine, L-methionine, and amino-DOI) and substrates (SAM and DOIA) indicated that the EPR signals observed during the reaction were derived from free BtrN, a BtrN−SAM complex, and a BtrN−SAM−DOIA complex. Significant changes in the EPR signals upon binding of SAM and DOIA suggest the close interaction of both substrates with the [4Fe-4S] cluster.

Oxidations of alcohols into carbonyl compounds are abundant in biological systems and often serve a central role in metabolism. These oxidation reactions generally proceed through a hydride transfer mechanism by nicotinamide-dependent dehydrogenases (*1–4*), flavin-dependent enzymes (*5, 6*), and pyrroloquinoline quinone-dependent dehydrogenases (*7, 8*). Only a few enzymes are known to catalyze oxidations of hydroxy groups through radical mechanisms, such as certain types of P450 oxidoreductases (*9–11*) and galactose oxidase (*12, 13*), which utilize dioxygen as an electron acceptor. Recently, we have found that a radical SAM[1] (*S*-adenosyl-L-methionine) enzyme, BtrN, catalyzes anaerobic oxidation of a hydroxy group into a ketone, namely, conversion of 2-deoxy-*scyllo*-inosamine (DOIA) into 3-amino-2,3-dideoxy-*scyllo*-inosose (amino-DOI), during biosynthesis of the 2-deoxystreptamine part of butirosin (Scheme 1) (*14*). The reaction of BtrN is quite unique because this enzyme utilizes SAM as the sole oxidant and does not require any extra electron acceptors. Similar anaerobic dehydrogenations by radical SAM enzymes were also reported for anaerobic sulfatase maturating enzymes (anSME), which catalyze post-transcriptional modifications of sulfatases by oxidizing serine or cysteine residues of sulfatases into formylglycines (*15, 16*). Although BtrN and anSME show little amino acid sequence homology, they both catalyze anaerobic oxidation of a hydroxy group without the assistance of other enzymes or an outside electron acceptor other than SAM (*14–16*). Thus, they can be defined as "radical SAM dehydrogenases" (*14*).

So far, mechanistic studies on these radical SAM dehydrogenases are quite limited. Our previous report revealed that the BtrN reaction consumes a stoichiometric amount of SAM and generates the corresponding amount of 5′-deoxyadenosine, L-methionine, and amino-DOI. The observation of deuterium atom transfer from the C-3 position of DOIA to 5′-deoxyadenosine indicated that the reaction proceeds through hydrogen atom abstraction by the 5′-deoxyadenosyl radical, which would generate a DOIA radical intermediate. Requirement of only 1 equiv of SAM for the oxidation of DOIA suggests the conversion of the putative DOIA radical intermediate to amino-DOI needs another electron acceptor. Since the reaction is independent of any outside electron acceptors for multiple turnovers, as described above, the $[4Fe\text{-}4S]^{2+}$ cluster of BtrN itself was proposed to accept the electron from the presumable DOIA radical

[†] This research was supported by Research Fellowships for Young Scientists from JSPS (K.Y.), the Naito Foundation (T.E.), a Grant-in-Aid for Scientific Research from JSPS, the Uehara Memorial Foundation, and the Noda Institute for Scientific Research (F.K.).

* To whom correspondence should be addressed: Department of Chemistry and Materials Science, Tokyo Institute of Technology, O-okayama, Meguro-ku, Tokyo 152-8551, Japan. E-mail: eguchi@cms.titech.ac.jp. Phone and fax: +81-3-5734-2631.

[‡] Department of Chemistry, Tokyo Institute of Technology.

[§] Juntendo University.

[‖] Department of Chemistry and Materials Science, Tokyo Institute of Technology.

[1] Abbreviations: SAM, *S*-adenosyl L-methionine; EPR, electron paramagnetic resonance; amino-DOI, 3-amino-2,3-dideoxy-*scyllo*-inosamine; DOIA, 2-deoxy-*scyllo*-inosamine; DOS, 2-deoxystreptamine; EDTA, ethylenediaminetetraacetic acid; HPLC, high-performance liquid chromatography; HEPES, 4-(2-hydroxyethyl)-1-piperazineethanesulfonic acid; anSME, anaerobic sulfatase maturating enzymes.

10.1021/bi800509x CCC: $40.75 
Published on Web 08/02/2008

Scheme 1: 2-Deoxystreptamine Biosynthesis in *Bacillus circulans*

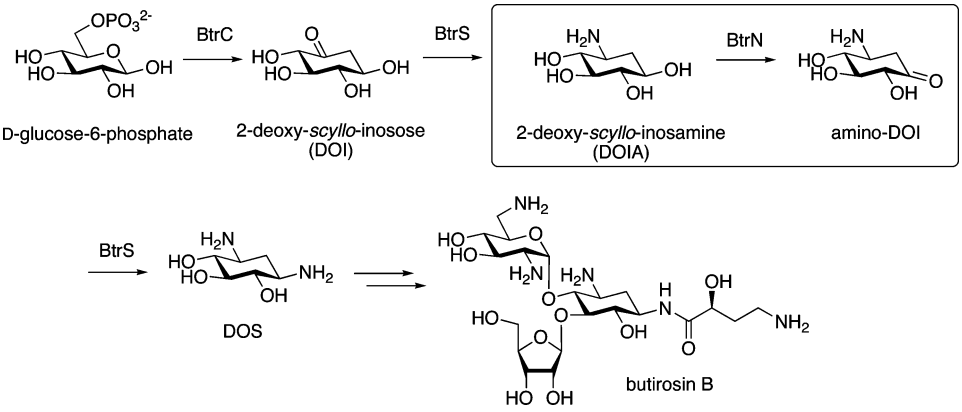


Scheme 2: Proposed Reaction Mechanism of BtrN

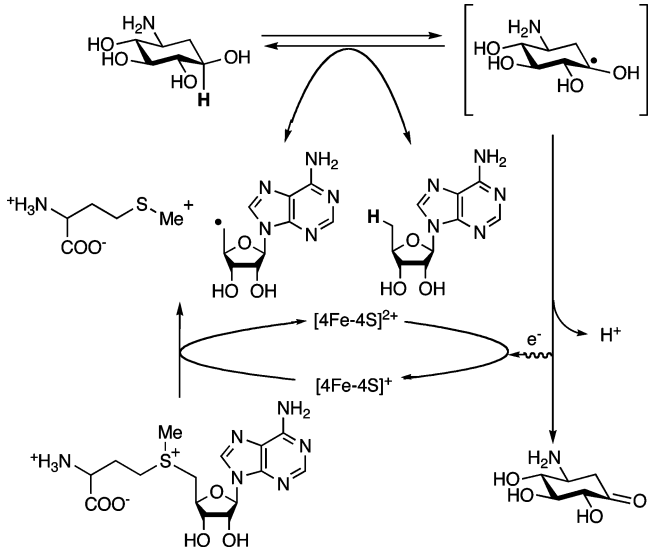


intermediate to complete the catalytic cycle (Scheme 2). Although the reaction by BtrN is unique and interesting, no spectroscopic evidence of a radical mechanism has been reported. In this work, to gain further insights into this intriguing enzyme, the BtrN reaction was analyzed by EPR spectroscopy and a radical intermediate derived from DOIA was successfully observed. This indicates a radical mechanism for the BtrN reaction. Further, the Fe−S cluster of BtrN during the reaction was also analyzed by EPR spectroscopy, which resulted in observation of signals derived from the 4Fe−4S cluster of free BtrN, a BtrN−SAM complex, and a putative BtrN−SAM−DOIA ternary complex. The significant changes in EPR spectra of the complexes indicate close interactions of SAM and DOIA with the 4Fe−4S cluster. This is the first report of an EPR study on the mechanism of radical SAM dehydrogenases.

## MATERIALS AND METHODS

*General Procedure.* HPLC was performed on a Hitachi L-6250 Intelligent Pump equipped with a Senshu Pak ODS 1251N column (4.6 mm × 250 mm, Senshu Scientific, Japan), an L-4000H UV detector, and a D-2500 Chromato-Integrator for the enzyme assay. $^1$H, $^2$H, and $^{13}$C NMR spectra were recorded with a JEOL Lambda-400 spectrometer or a Bruker DRX-500 spectrometer. Deuterium oxide (Merck, 99.9 at. % enriched) was used as an NMR solvent. Chemical shifts are reported in $\delta$ values based on the solvent signal ($D_2O$ $\delta_H = 4.65$) as a reference. Dioxane ($\delta_C = 66.5$) was used an internal standard for $^{13}$C NMR. UV−vis absorption spectra were recorded with a DU7400 spectrophotometer (Beckman). Other chemicals were of the highest grade commercially available.

*Preparation of BtrN.* BtrN was overexpressed in *Escherichia coli*, anaerobically purified, and reconstituted in vitro as previously reported (*14*) with minor modifications. All buffer solutions were degassed with a freeze−thaw procedure under reduced pressure, followed by bubbling with a mixture of argon and hydrogen gas purified through a reduced Cu catalyst. The purified BtrN (~0.07 mM) was reconstituted with $Na_2S$ (0.67 mM) and $Fe^{II}(NH_4)_2(SO_4)_2$ (0.67 mM) and incubated for 40 min at room temperature. Excess Fe ion was trapped by addition of EDTA (0.85 mM) and desalted with a Hi-trap desalting column (Amersham Pharmacia Biotech) to prepare the reconstituted BtrN. Protein concentrations were determined with the Bio-Rad protein assay (Bio-Rad) using bovine plasma $\gamma$-globulin as a standard. Enzymes were freshly prepared for each set of experiments. The DOIA oxidation activity of BtrN was confirmed as follows. BtrN (0.18−0.23 $\mu$M) was incubated with DOIA (0.1 mM) and varied concentrations of SAM (0.03, 0.05, 0.1, 0.2, 0.4, 0.8, and 1.6 mM) in 50 mM HEPES-NaOH (pH 8.0) in the presence of sodium dithionite (10 mM) at room temperature for 0.5 h. The reaction was quenched with 10% trichloroacetic acid, and the generated 5′-deoxyadenosine was quantitated by HPLC as previously reported (*14*). Reactions were run in duplicate, and the data were fitted to the Michaelis−Menten equation [$v$/[BtrN] = $k_{cat}$[SAM]/($K_M$ + [SAM])] by a least-squares method.

*Determination of the Iron Content.* The quantitation of the iron content was conducted using the reported procedure (*17*). A BtrN solution (200 $\mu$L, without sodium dithionite) was treated with 100 $\mu$L of reagent A (2.25% $KMnO_4$ in 0.6 N aqueous HCl) at 60 °C for 2 h, followed by the addition of 20 $\mu$L of reagent B (8.8 g of ascorbate, 9.7 g of ammonium acetate, 80 mg of ferrozine, and 80 mg of neocuproine dissolved in 25 mL of water), and the mixture was incubated for 1 h at room temperature. Absorption at 562 nm was measured, and the iron concentrations of the samples were determined according to the standard curve generated by 10−50 $\mu$M $Fe^{II}(NH_4)_2(SO_4)_2$.

*Preparation of 2-Deoxy-scyllo-[2,2-$^2H_2$]inosamine.* Hexokinase (1.5 mg), ATP (60.6 mg, 5.5 mM), $MgCl_2$ (20 mg,

5 mM), and D-[6,6-$^2H_2$]glucose (18 mg, 5 mM) were incubated in 20 mL of 50 mM HEPES-NaOH (pH 8.0) at 37 °C for 30 min. Then, $NAD^+$ (20 mg), 2-deoxy-*scyllo*-inosose (DOI) synthase (BtrC, 20 $\mu$M), and $CoCl_2$ (1.25 mM) were added, and the reaction mixture was further incubated at 37 °C for 30 min. After removal of the precipitate by centrifugation, the reaction mixture was applied to an Amberlite CG50 ($H^+$ form) column and the unabsorbed fraction was collected. After the pH of the solution had been adjusted to 8.0 with 0.2 M aqueous NaOH, L-glutamine:DOI aminotransferase (BtrS, 20 $\mu$M), PLP (0.5 mM), and L-glutamine (10 mM) were added, and the mixture was incubated at room temperature for 4 h. The precipitate was removed by centrifugation, and the supernatant was applied to an Amberlite CG50 ($NH_4^+$ form) column. The column was washed with 50 mM $NH_4OH$, and DOIA was then eluted with 200 mM $NH_4OH$. The solvent was removed in vacuo with a rotary evaporator, and the counteranion was exchanged with chloride when the sample was passed through a DOWEX AG1X8 ($Cl^-$ form) column to yield 2-deoxy-*scyllo*-[2,2-$^2H_2$]inosamine hydrochloride (8.2 mg, 92 at. % D): $^1$H NMR (400 MHz, $D_2O$) $\delta$ 3.09 (d, $J$ = 10.4 Hz, 1H), 3.20 (t, $J$ = 6.8 Hz, 1H), 3.22 (t, $J$ = 6.9 Hz, 1H), 3.35−3.43 (m, 1H), 3.49−3.55 (m, 1H); $^{13}$C NMR (125 MHz, $D_2O$) $\delta$ 31.64 (q, $J$ = 22 Hz), 49.72, 68.4, 72.8, 74.3, 76.1; $^2$H NMR (61 MHz, $D_2O$) $\delta$ 1.43, 2.12.

*Preparation of Amino-DOI.* BtrS (50 $\mu$M) was incubated with 2-deoxystreptamine (4 mM, 18.4 mg), pyruvate (100 mM, 220 mg), and PLP (0.5 mM) in 20 mL of 50 mM HEPES-NaOH (pH 8.0) at 28 °C for 3 h. After removal of the enzyme by ultrafiltration, the solution was applied to a DOWEX AG1X8 (acetate form) column and the unadsorbed fraction was collected. The resultant filtrate was applied to an Amberlite CG50 ($H^+$ form) column, and the column was washed with water. Then, elution was carried out with a linear gradient from 0 to 100 mM aqueous HCl (total of 300 mL). Amino-DOI was eluted at 20−33 mM HCl, and the solvent was removed in vacuo. The residue was further purified with Sephadex G-10 (100 mL, 1.0 cm × 120 cm) to remove inorganic salt. The elution was carried out with water to yield pure amino-DOI (3.7 mg). Hydrate form: $^1$H NMR (400 MHz, $D_2O$) $\delta$ 1.70 (t, $J$ = 12.0 Hz, 1H, H-2ax), 2.14 (dd, $J$ = 4.4, 12.0 Hz, 1H, H-2eq), 3.13 (ddd, $J$ = 4.4, 10.2, 12.0 Hz, 1H, H-3), 3.30−3.43 (m, 3H, H-4, -5, -6); $^{13}$C NMR (125 MHz, $D_2O$) $\delta$ 36.57, 49.96, 72.92, 73.79, 75.78, 92.88; HR-FAB-MS (positive, glycerol) *m/z* 180.0872 $(M + H)^+$, calcd for $C_6H_{14}O_5N$ 180.0872. Ketone form: $^1$H NMR (400 MHz, $D_2O$) $\delta$ 2.81−2.86 (m, 2H, H-2), 3.30−3.43 (m, 2H, H-3, -5), 3.94 (dd, $J$ = 9.5, 10.5 Hz, 1H, H-4), 4.29 (d, 1H, H-6); $^{13}$C NMR (125 MHz, $D_2O$) $\delta$ 39.48, 49.41, 72.01, 74.36, 77.57, 204.2; IR (KBr) 3490, 1645, 1196 (shoulder), 1090, 959, 797 cm$^{-1}$; HR-FAB-MS (positive, glycerol) *m/z* 162.0769 $(M + H)^+$, calcd for $C_6H_{12}O_4N$ 162.0766.

*EPR Measurements.* The reconstituted BtrN was reduced with sodium dithionite (10 mM) at room temperature for 1 h and incubated with substrates or products in 50 mM HEPES-NaOH (pH 8.0). For EPR measurements during the catalytic cycle, BtrN (35 $\mu$M) was incubated with SAM (1 mM) and DOIA (1 mM) in the presence of sodium dithionite (10 mM) at room temperature, and the reaction was freeze-quenched in liquid nitrogen at set time points (3, 10, 20, 40, and 60 min). When deuterated DOIA was used as a substrate, BtrN (21 $\mu$M) was incubated with SAM (1 mM) and DOIA (1 mM) in the presence of sodium dithionite (10 mM) at room temperature for 10 min before the reaction was freeze-quenched in liquid nitrogen. For EPR measurements of the BtrN−substrate and BtrN−product complexes, BtrN was incubated with substrates (SAM and DOIA) and/or products (5′-deoxyadenosine, L-methionine, and amino-DOI) at room temperature for 20 min and freeze-quenched in liquid nitrogen. The precise conditions, including enzyme concentrations and combinations of additives, are described in the legend of each figure. EPR spectra were recorded with a JEOL JES-FA300 ESR spectrometer (9.02 GHz). Recording conditions are indicated in the legend of each figure. EPR simulation was achieved using AniSimu/FA version 2.0.0 (JEOL). Quantitation of the EPR signals was achieved by comparison of the double integrals with those of a standard sample of 0.01 $\mu$mol of $CuSO_4$.

*Reverse Reaction of BtrN.* Amino-DOI (2 mM) was incubated with BtrN (17 $\mu$M), L-methionine (5 mM), 5′-deoxyadenosine (5 mM), and sodium dithionite (10 mM) in 50 mM HEPES-NaOH (pH 8.0) at 28 °C for 12 h. An aliquot (20 $\mu$L) of the mixture was treated with 20 $\mu$L of 5% 2,4-dinitrofluorobenzene in methanol, 10 $\mu$L of DMSO, and 2 $\mu$L of 2 M NaOH at 60 °C for 1 h. The solvent was then removed in vacuo and redissolved in 0.1 mL of methanol. The resultant mixture was diluted with 3 mL of water and passed through the Sep-Pak C-18 cartridge (Waters). The cartridge was washed with 7 mL of water, and the product, 2,4-dinitrophenyl-DOIA, was eluted with 5 mL of methanol. After removal of the solvent by a centrifugal evaporator, the residue was dissolved in 100 $\mu$L of methanol. An aliquot (5 $\mu$L) of the solution was injected into the same HPLC system as described above and eluted with 30% aqueous methanol at a flow rate of 0.9 mL/min at room temperature. The eluent was monitored at 350 nm.

## RESULTS

*Determination of the BtrN Iron Content.* Before the precise mechanistic studies by EPR, the Fe content of BtrN was determined. Fe quantitation of BtrN prepared with the previously reported procedure resulted in large and variable values for the amount of Fe (10−20 Fe atoms per polypeptide). We presumed that this is due to FeS precipitation and/or nonspecifically bound Fe copurified with BtrN by gel filtration after reconstitution. To prevent this phenomenon, the reconstituted BtrN was treated with EDTA to remove those excess iron ions. Expression and purification of BtrN were conducted as previously reported. Purified BtrN was then incubated with Fe(II) (0.67 mM) and $Na_2S$ (0.67 mM) for 40 min at room temperature, and the excess Fe ion was trapped by addition of a slight excess of EDTA (0.85 mM) and removed by gel filtration. Since the use of EDTA in Fe−S reconstitution includes the risk of losing the weakly bound Fe−S cluster required for an enzyme activity, as is the case for MiaB (*18*), the specific activity of the reconstituted BtrN was measured. The apparent kinetic constant of EDTA-treated BtrN ($K_{M,SAM,app}$ = 0.31 ± 0.12 mM and $k_{cat,app}$ = 1.3 ± 0.10 min$^{-1}$ at 0.1 mM DOIA; see the Supporting Information for data sets) and the previously reported value obtained for BtrN reconstituted without the addition of EDTA

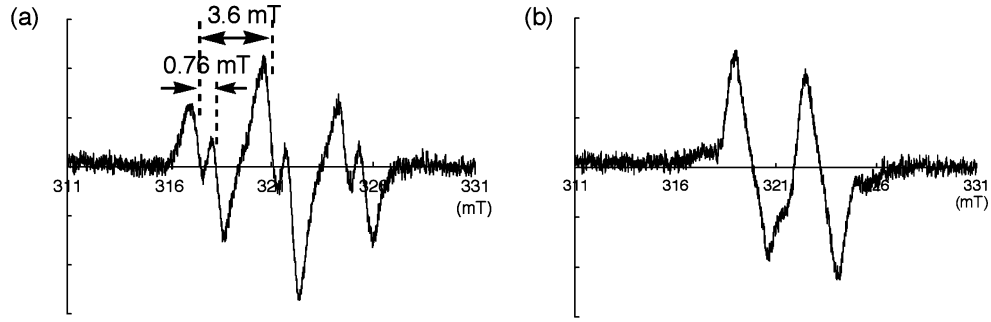


FIGURE 1: EPR spectra of the BtrN reaction. (a) EPR spectrum of the BtrN reaction recorded at 50 K with a microwave power of 0.4 mW. BtrN (35 $\mu$M) was incubated with DOIA (1 mM), SAM (1 mM), and sodium dithionite (10 mM) in 50 mM HEPES-NaOH (pH 8.0) at room temperature for 10 min, and the mixture was freeze-quenched manually in liquid nitrogen. (B) EPR spectrum of the BtrN reaction using [2,2-$^2H_2$]DOIA recorded at 50 K with a microwave power of 0.4 mW. BtrN (21 $\mu$M) was incubated with [2,2-$^2H_2$]DOIA (1 mM), SAM (1 mM), and sodium dithionite (10 mM) in 50 mM HEPES-NaOH (pH 8.0) at room temperature for 10 min and flash-frozen in liquid nitrogen. Recording conditions: modulation width, 0.6 mT; modulation frequency, 100 kHz; microwave power, 0.4 mW. Averages of four scans were used.

Scheme 3: Preparation of [2,2-$^2H_2$]DOIA

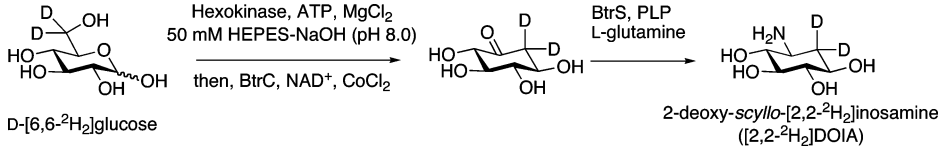


($K_{M,SAM,app}$ = 0.46 ± 0.10 mM, and $k_{cat,app}$ = 1.2 ± 0.10 $min^{-1}$ at 0.1 mM DOIA) (*14*) were identical within the range of error. This result suggests that, in this case, EDTA treatment removed only FeS precipitation and/or nonspecifically bound Fe ions, which could not be removed by gel filtration. The iron quantitation of the prepared BtrN resulted in 4.0 ± 0.1 iron ions per monomer. The EPR signal of BtrN reconstituted with EDTA exhibited an axial signal (Figures 4 and 5) identical to the previous report (*14*). Spin quantitations of the signal resulted in 0.4−0.6 spin per monomer. Fluctuation in the spin amount is probably due to incomplete reduction, which was also observed for other radical SAM enzymes (*19, 20*). All these results indicate that BtrN has one [4Fe-4S]$^+$ cluster per monomer.

*Observation of an Organic Radical Intermediate.* To analyze the BtrN reaction by EPR spectroscopy, the reduced BtrN (35 $\mu$M protein with 17.5 $\mu$M spins) was incubated with SAM (1 mM) and DOIA (1 mM) in the presence of sodium dithionite (10 mM) at room temperature for 10 min and the mixture was flash-frozen manually in liquid nitrogen. The EPR spectrum was first recorded at 50 K to detect signals of organic radical species. As a result, a sharp double triplet signal with hyperfine coupling constants of 0.76 ± 0.02 and 3.6 ± 0.3 mT was observed at $g$ = 2.0025 ± 0.0005 (Figure 1a). According to power saturation experiments, the signal was not saturated under this condition (data not shown). The spin concentration was estimated to be 0.14 $\mu$M by comparing a double integral of the signal with a standard Cu(II)$SO_4$. This signal was not observed when either of the substrates or BtrN was omitted, indicating this signal is derived from a reaction intermediate. According to the hyperfine structure, the signal was presumed to be that of the DOIA radical intermediate. To further characterize the signal, deuterated DOIA was prepared and used for the EPR measurement.

2-Deoxy-*scyllo*-[2,2-$^2H_2$]inosamine ([2,2-$^2H_2$]DOIA, 92 at. % D) was prepared from D-[6,6-$^2H_2$]glucose using hexokinase, 2-deoxy-*scyllo*-inosose synthase (BtrC) (*21*), and 2-deoxy-*scyllo*-inosose:L-glutamine aminotransferase (BtrS) (*22*) (Scheme 3). Metals used for the reaction of hexokinase and BtrC were removed when the resultant solution was passed through an Amberlite CG50 column ($H^+$ form) prior to the reaction with BtrS. The obtained [2,2-$^2H_2$]DOIA (1 mM) was subjected to reaction with BtrN (21 $\mu$M) and SAM (1 mM), and the EPR spectrum was recorded at 50 K. As a result, the spin coupling with protons partially disappeared and a doublet signal with a hyperfine coupling constant of 3.7 ± 0.3 mT was observed (Figure 1b), which unambiguously proves the generation of a radical on C-3 of DOIA.

For $\beta$-proton splitting, a hyperfine coupling constant, $A$, is known to depend on a dihedral angle, $\theta$, defined in Figure 2a with the following relationship (*23, 24*):

$$A(\theta) = \rho(B_0 + B\cos^2\theta)$$

where $B_0$ is the hyperfine coupling constant via a $\sigma$ bond per unit electron density on Cα, $B$ is the hyperfine coupling constant through hyperconjugation per unit electron density on Cα, and $\rho$ is the electron density on Cα.

Generally, the contribution of hyperfine coupling via a $\sigma$ bond is small (<0.1 mT) and negligible. A value of 5.8 mT for $B$, empirically obtained from the experimental data of various alkyl radical species, was used (*23, 25, 26*). First, $\theta$ values for the C-2 protons were calculated. Considering that C-2 is an $sp^3$ center, the difference in the $\theta$ value between two protons on C-2 can be assumed to be 120°. Since $\theta$ is set between 0° and 180°, and $\rho$ should be between 0 and 1, two simultaneous equations obtained by substitution of $A(\theta)$ with 3.7 ± 0.3 and 0.77 ± 0.02 mT gave two possible $\theta$ values: 63 ± 1° (Figure 2b, left) and 178 ± 2° (Figure 2b, right), respectively, which both gave the same $\rho$ value (0.63 ± 0.04). Thus, using this $\rho$ value and the coupling constant between the electron and the C-4 proton, 3.7 ± 0.3 mT, the $\theta$ for the C-4 proton was determined to be 0 ± 4°. According to this $\theta$ value of the C-4 proton, the $\theta$ value of C-2 protons can be reasonably determined to be 63 ± 1° (Figure 2b, left) because of the conformational constraint of the cyclohexane

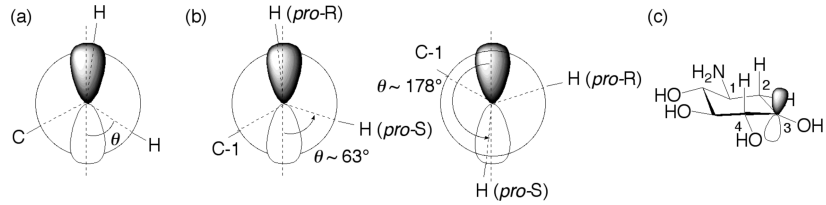


FIGURE 2: (a) Dihedral angle responsible for the $\beta$-proton splitting. (b) Two possible relative conformations of the C-2−C-3 bond. (c) One conformation of the DOIA radical predicted from the hyperfine coupling constants.

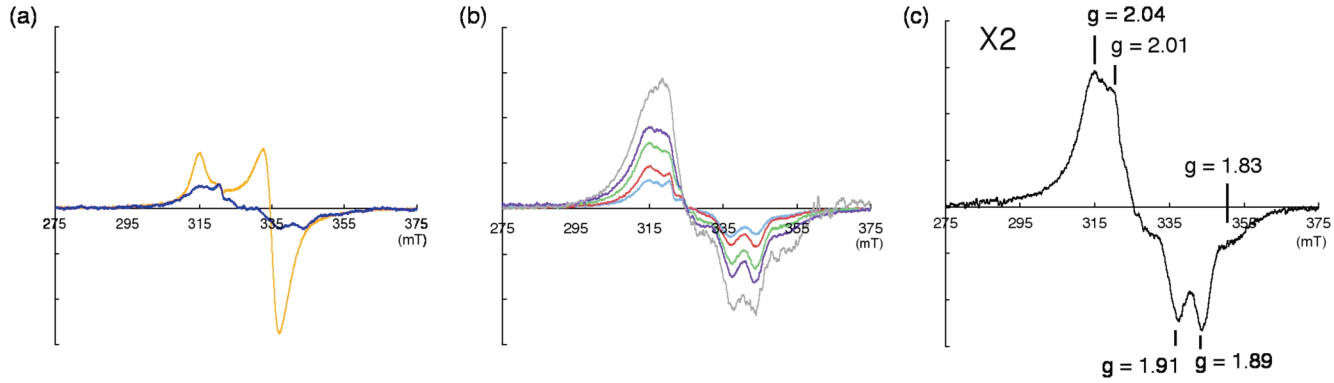


FIGURE 3: EPR spectra of the BtrN reaction mixture recorded at 10 K. The sample used in this figure was identical to that used for Figure 1a. (a) Overlay of the EPR spectrum of the BtrN reaction mixture with the spectrum of BtrN before the addition of SAM and DOIA (orange line). Both spectra were recorded at a microwave power of 1 mW. (b) Power saturation experiments of the EPR signal of the BtrN reaction mixture: light blue, 1 mW; red, 2 mW; green, 8 mW; blue, 16 mW; gray, 64 mW. (c) EPR spectrum recorded with a microwave power of 8 mW. Scaling was magnified 2-fold for clarity. Other recording conditions: temperature, 10 K; modulation width, 0.6 mT; modulation frequency, 100 kHz.

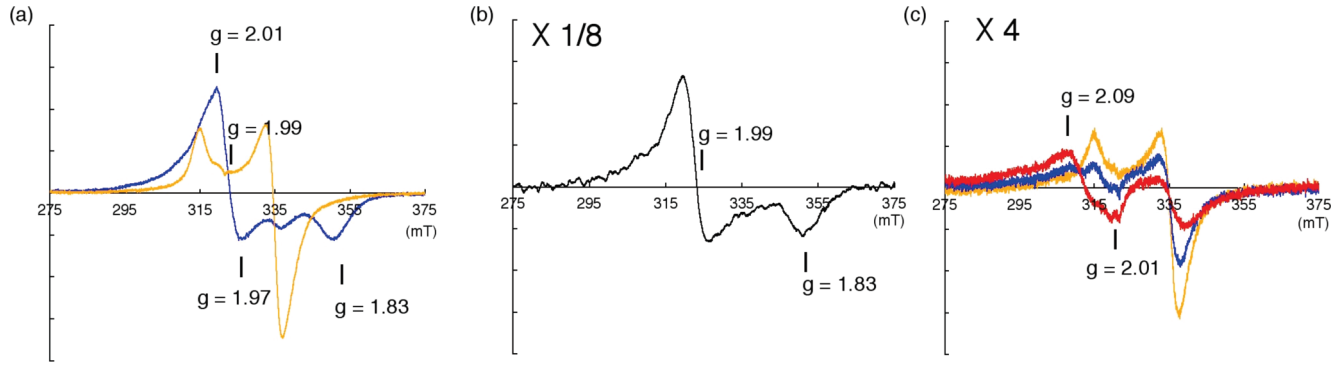


FIGURE 4: (a) Overlay of EPR spectra of the reduced BtrN (35 $\mu$M) incubated with SAM (1 mM) (blue line) and the reduced BtrN (35 $\mu$M) before addition of SAM (orange line). Recording conditions: microwave power, 1 mW; temperature, 10 K; modulation width, 0.6 mT; modulation frequency, 100 kHz. Spectra were averages of four scans. (b) EPR spectrum of BtrN (35 $\mu$M) incubated with SAM (1 mM) recorded at a microwave power of 64 mW. The scaling was reduced to 1/8. Other recording conditions were identical to those described for panel a. (c) Overlay of EPR spectra of BtrN (10 $\mu$M) incubated with DOIA (1 mM) recorded at 10 K (blue line) and 5 K (red line) and the EPR spectrum of BtrN (10 $\mu$M) before addition of DOIA (orange line). The scaling was magnified 4-fold. Other recording conditions were identical to those described for panel a.

ring. These results suggest the p$\pi$ orbital of the isolated electron and the axial protons have almost an eclipse conformation as shown in Figure 2c.

*EPR Signal for the 4Fe−4S Cluster during the Catalytic Cycle.* The EPR spectrum of the reaction mixture [BtrN (35 $\mu$M protein with 17.5 $\mu$M spins) with DOIA (1 mM), SAM (1 mM), and sodium dithionite (10 mM), incubated for 10 min at room temperature] described above was also recorded at 10 K. As a result, the EPR signal for the [4Fe-4S]$^+$ cluster was significantly decreased from that of the unreacted [4Fe-4S]$^+$ cluster of BtrN (Figure 3a), and its shape was also dramatically changed. The $g$ = 2.01 (320 mT) peak is a saturated broadened signal of the DOIA radical intermediate. To reduce the contribution of this signal, signals of the Fe−S cluster were amplified by increasing the microwave power. Power saturation experiments indicated that the spin relaxation of the signals presumably derived from the Fe−S cluster was not saturated at least up to the microwave power of 8 mW at 10 K, while the feature at 320 mT became negligible under this condition (Figure 3b,c). The obtained signal had new features [$g$ = 1.83, 1.89, 2.01, and 2.04 (Figure 3c)]. The signal seemed to be a mixture of several chemical species and was quite difficult to interpret at this point. To assign these signals, the effects of addition of substrate and product on the EPR signal were examined.

The EPR signal of BtrN (35 $\mu$M) incubated with SAM (1 mM) dramatically changed from that of free BtrN (Figure 4a). The newly generated signal had a shorter spin relaxation time and could be distinguished from the signal of free BtrN by increasing the microwave power (Figure 4b; see the

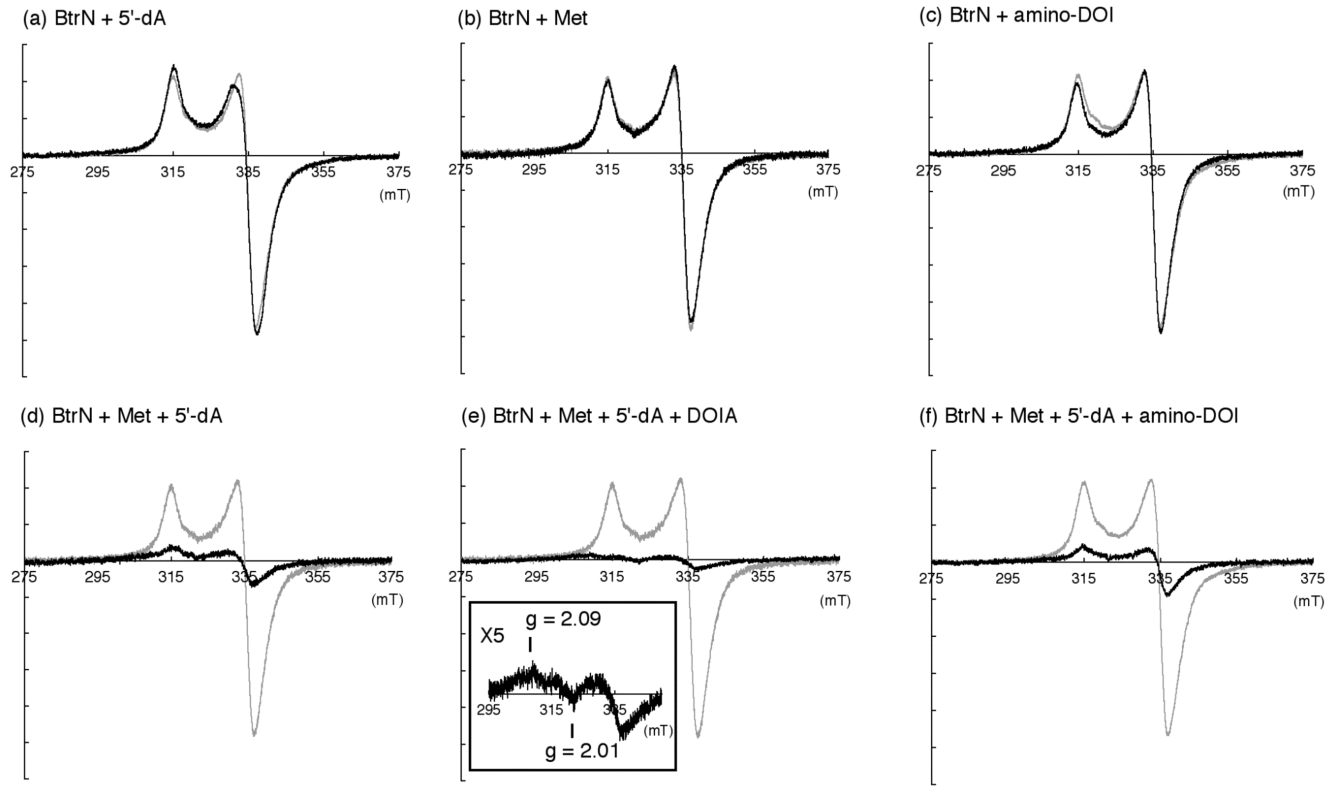


FIGURE 5: EPR spectra of BtrN (30 $\mu$M) incubated with (a) 5′-deoxyadenosine, (b) L-methionine, (c) amino-DOI, (d) L-methionine and 5′-deoxyadenosine, (e) L-methionine, 5′-deoxyadenosine, and DOIA, and (f) L-methionine, 5′-deoxyadenosine, and amino-DOI. BtrN was incubated with additives (each compound at 1 mM) for 20 min at room temperature and flash-frozen in liquid nitrogen. Grey lines are the EPR spectra before the incubation with the additives. Recording conditions: modulation width, 0.6 mT; temperature, 10 K; microwave power, 1 mW. Spectra are averages of four scans. Signal intensities were normalized according to the spin amount of free BtrN since it differed upon enzyme preparations. BtrN with 0.4 spin per monomer was used for panels b, d, and e, and BtrN with 0.6 spin per monomer was used for panels a, c, and f.

Supporting Information for power saturation experiments). From these experiments, the signal generated by SAM addition was shown to have an axial feature with $g$ values of 1.83 and 1.99.

The addition of DOIA also showed a new $g = 2.01$ and 2.09 feature (Figure 4c). The intensity of the signal was increased at 5 K, suggesting that its spin relaxation is faster than that of the free BtrN, which exhibited the highest intensity at 10 K (see the Supporting Information). Even though the substrate/enzyme ratio was increased 3.5-fold, only approximately 30% of the signal derived from the free BtrN disappeared (Figure 4c). These results suggest that DOIA can also bind to the enzyme active site near the cluster independently, but rather weakly relative to SAM.

The effects of product binding on the EPR signal of the 4Fe−4S cluster were also examined. BtrN (30 $\mu$M) was incubated with amino-DOI, L-methionine, 5′-deoxyadenosine, or their mixture and was analyzed by EPR (Figure 5). The concentration of each additive was uniformly adjusted to 1 mM, which is the maximum concentration possible in the BtrN reaction mixture described in the legends of Figures 1 and 3. Amino-DOI was prepared by deamination of 2-deoxystreptamine by BtrS (*27, 28*) using pyruvate as an amino acceptor as described in Materials and Methods. Amino-DOI could be isolated in the hydrochloride form without further derivatizations, and its structure was confirmed by NMR, HR-FAB-MS, and IR spectroscopy. The isolated amino-DOI existed in both keto and hydrate form in a water solution, which was also the case for 2-deoxy-*scyllo*-inosose (*29*). When amino-DOI, L-methionine, or 5′-deoxyadenosine was separately added to a BtrN solution, a significant effect was not observed on the EPR signal of the cluster at all (Figure 5a−c). Only 5′-deoxyadenosine exhibited a small perturbation for the $g = 1.93$ peak (Figure 5a). Power saturation experiments with the 5′-deoxyadenosine-supplemented BtrN solution showed that the signal was already saturated under this condition (data not shown), which should be the cause of the change in the shape of the spectrum. On the other hand, a significant decrease in signal intensity was observed when L-methionine and 5′-deoxyadenosine were added simultaneously (Figure 5d). No new signal for the Fe−S cluster or organic radical species was observed even in the lower magnetic field area at temperatures of 5−80 K and microwave powers of 0.1−50 mW. The addition of DOIA (Figure 5e) or amino-DOI (Figure 5f) to this mixture did not generate any new signals except for $g = 2.01$ and 2.09 features, which were also observed in the independent incubation of DOIA with reduced BtrN (Figure 4c). Again, no organic radical was observed in these mixtures. Since the UV−vis absorption spectrum of the 4Fe−4S cluster was not changed upon addition of L-methionine and 5′-deoxyadenosine (Figure 6), it seemed unlikely that the oxidation of the $[4Fe\text{-}4S]^{+}$ cluster to a $[4Fe\text{-}4S]^{2+}$ cluster occurred under this condition. This signal decrease caused by L-methionine and 5′-deoxyadenosine binding is discussed below.

Comparing the EPR signals observed during the catalytic cycle (Figure 3c) with the EPR signals of BtrN incubated

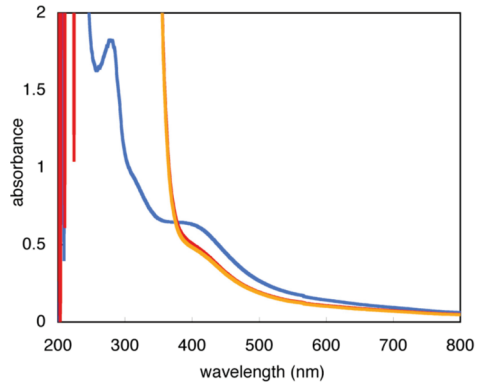


FIGURE 6: UV−vis spectra of BtrN: (blue line) as-reconstituted BtrN (24 $\mu$M), (red line) BtrN (24 $\mu$M) reduced with dithionite (10 mM) for 30 min at room temperature, (yellow line) BtrN (24 $\mu$M) reduced with dithionite (10 mM) for 30 min at room temperature, followed by incubation with L-methionine (1 mM) and 5′-deoxyadenosine (1 mM) for 30 min at room temperature.

with various combinations of substrates and products (Figures 4 and 5), we can identify the $g = 1.91$ feature observed during the reaction as the signal of free BtrN and the $g = 1.83$ and 2.01 features as the signal of the SAM-bound 4Fe−4S cluster of BtrN (Figures 3c and 4a,b). On the other hand, $g = 1.89$ and 2.04 features were observed only during the catalytic cycle. To further characterize these signals, signals of free BtrN and the BtrN−SAM complex were subtracted from the signal observed during the catalytic cycle (Figure 3c). The signal of the BtrN−SAM complex was subtracted so that the $g = 1.83$ feature became flat. The signal of free BtrN was subtracted to make the $g = 1.91$ feature negligible. The spectra of free BtrN and the BtrN−SAM complex used for the subtraction were both recorded under the same conditions as the experiment described for Figure 3c. As a result, the spectrum of free BtrN with 0.5 $\mu$M spins (7% of the spectrum containing 7.1 $\mu$M spins) and the spectrum of the BtrN−SAM complex with 1.8 $\mu$M spins (18% of the spectrum containing 10 $\mu$M spins) were subtracted, and a rhombic signal with $g$ values of 1.87, 1.96, and 2.05 was obtained (Figure 7). The spin concentration of this rhombic signal was estimated to be 2.1 $\mu$M. This signal was observed only in the presence of the both substrates, and not observed in other combinations of substrates or products. Thus, the rhombic signal should be derived from an intermediate after the formation of the BtrN−SAM complex and before the formation of the BtrN−amino-DOI−5′-deoxyadenosine−methionine quaternary complex (Scheme 4). Considering the catalytic role of the 4Fe−4S cluster, the initial $[4Fe\text{-}4S]^{+}$ cluster should be oxidized to a $[4Fe\text{-}4S]^{2+}$ cluster and become EPR silent upon reductive cleavage of SAM until the oxidized cluster is reduced somehow by the DOIA radical, which should generate the BtrN−amino-DOI−5′-deoxyadenosine−methionine quaternary complex (Schemes 2 and 4). Since the incubation of BtrN with 5′-deoxyadenosine, L-methionine, and amino-DOI did not result in generation of such a rhombic signal, the signal cannot be derived from the BtrN−amino-DOI−5′-deoxyadenosine−methionine quaternary complex. Thus, a BtrN−SAM−DOIA ternary complex is the only one possible EPR active intermediate left uncharacterized, and it is reasonable to assign the rhombic signal as the BtrN−SAM−DOIA ternary complex.

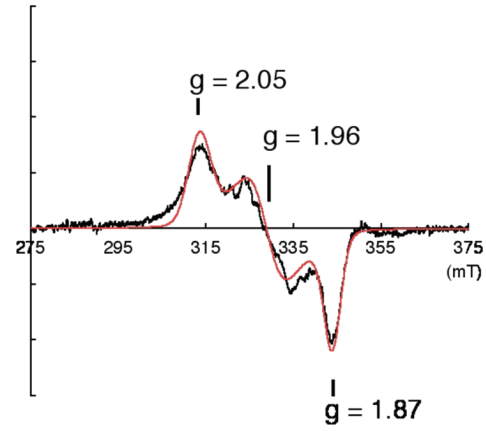


FIGURE 7: EPR spectrum obtained after subtraction of the signals of the free BtrN (0.5 $\mu$M spins) and the BtrN−SAM complex (1.8 $\mu$M spins) from the spectrum observed during catalytic turnover. The spectra of free BtrN and the BtrN−SAM complex were recorded under the same condition described in the legend of Figure 3c. The red line represents a simulated curve. The following parameters were used: $g = 1.87$, 1.96, and 2.05; Lorentzian ratio of 20% and Gaussian ratio of 80%; spectrum widths $\Sigma_X = 3.80$ mT, $\Sigma_Y = 7.00$ mT, and $\Sigma_Z = 5.00$ mT.

The time course of the intensities of the signals observed during catalytic turnover was shown in Figure 8. The spin concentrations of the rhombic signal were estimated by comparison of a double integral of each signal with that of the $Cu(II)SO_4$ standard. The signal of the DOIA radical showed the highest intensity at 3 min and became almost constant after 20 min, which suggests the presteady state accumulation of DOIA radical (Figure 8a,b). The spin concentration of the rhombic signal was estimated from the comparison of peak-to-peak intensity of the $g = 1.89$ and 2.04 features with that of the signal shown in Figure 3a whose concentration was determined to be 2.1 $\mu$M as described above. As a result, the spin concentrations of the rhombic signal were also highest at the beginning of the reaction (Figure 8c,d). The reaction was repeated twice, and similar presteady state accumulations of both signals were observed in all experiments. Presteady state accumulation of the rhombic signal suggests that the signal is derived from an intermediate before the rate-determining step, presumably ketone formation, which is consistent with the assignment of the rhombic signal as the BtrN−SAM−DOIA complex.

Furthermore, when the incubation was continued for more than 60 min, we observed a decrease in both signals after 120 min and almost complete disappearance after 240 min (see the Supporting Information). We have previously reported that when BtrN (30 $\mu$M) was incubated with DOIA (1 mM) and SAM (0.9 mM) for 240 min at room temperature, more than 70% of DOIA was converted into amino-DOI and the reaction rate dramatically decreased (*14*). Since the reaction condition in this paper is similar to those of the previous report, disappearance of both signals by completion of the reaction further supports the possibility that both signals are derived from reaction intermediates. Disappearance of the 4Fe−4S cluster signal should be due to the accumulation of the BtrN−amino-DOI−5′-deoxyadenosine−methionine or BtrN−5′-deoxyadenosine−methionine complex, whose 4Fe−4S clusters were shown to be difficult to detect by EPR.

Scheme 4: BtrN Reaction Mechanism Revealed by EPR Experiments

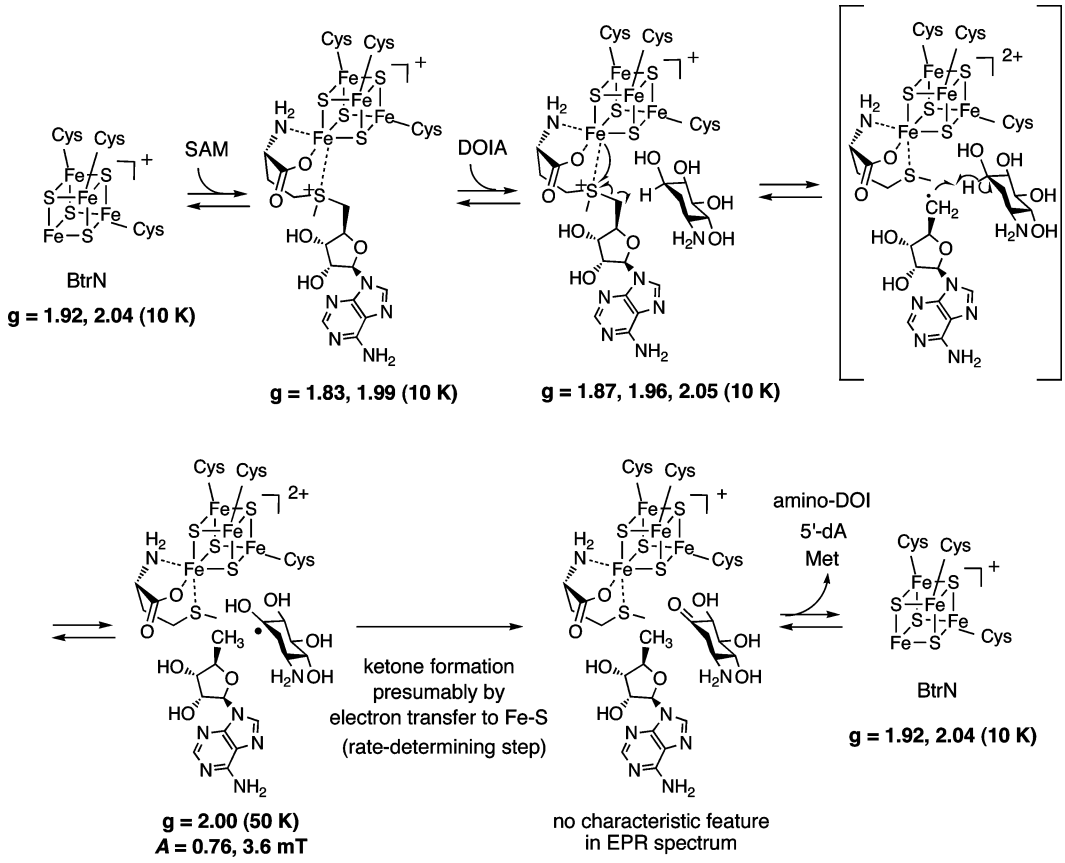


## DISCUSSION

BtrN is a radical SAM dehydrogenase catalyzing DOIA oxidation coupled with reductive cleavage of SAM. To gain further insights into the reaction mechanism, we first characterized the Fe−S cluster of BtrN. The results of Fe quantitation resulted in 4.0 ± 0.1 irons per polypeptide, and EPR spin quantitation showed 0.4−0.6 spin per monomer. Although BtrN has five cysteines other than those of the radical SAM 4Fe−4S cluster motif, they are not conserved in other Fe−S cluster proteins, and no other motifs for the Fe−S cluster were found. Thus, our results indicate the presence of only one 4Fe−4S cluster per BtrN subunit. However, considering that some radical SAM enzymes have multiple Fe−S clusters in a single subunit (*15, 18, 30–32*), Mössbauer experiments might be required for a more accurate characterization of the cluster composition.

From the BtrN reaction solution containing SAM and DOIA, an EPR signal derived from the DOIA radical intermediate was observed at 50 K. The observation of the radical intermediate strongly supports the previously proposed radical mechanism (Scheme 2). The time course of the signal intensity showed the accumulation of the DOIA radical during the presteady state, which lasted for at least 20 min under this condition (Figure 8). This long presteady state is consistent with a slow reaction rate of BtrN (~0.2 $min^{-1}$ under this condition). Considering that the incubation of BtrN with 5′-deoxyadenosine, L-methionine, and amino-DOI did not generate a detectable amount of DOIA radical (Figure 5) or DOIA itself (see the Supporting Information), ketone formation should be an irreversible reaction. Thus, the accumulation of the DOIA radical intermediate during the presteady state suggests that ketone formation is the rate-determining step in this reaction. The slow rate of ketone formation is consistent with the previously reported accumulation of deuterium in 5′-deoxyadenosine and small kinetic isotope effect observed when [3-$^2$H]DOIA was used as a substrate (*14*).

The observed DOIA radical should be further oxidized via the release of an electron and a proton to generate amino-DOI. Since the reaction proceeds without addition of external electron acceptors, the $[4Fe\text{-}4S]^{2+}$ cluster was proposed to be the final electron acceptor (*14*). The observed DOIA radical can easily be converted to a highly reductive ketyl radical by deprotonation (for example, cyclohexanone has −2.2 V) (*33*), which should be sufficient to reduce the $[4Fe\text{-}4S]^{2+}$ cluster (−0.4 to −0.5 V) (*34*). Since $pK_a$ values of aliphatic ketyl radicals are generally 3−5 units lower than those of their corresponding alcohols (for example, $pK_a$ = 16 for cyclohexanol and $pK_a$ = 12.1 for cyclohexanone ketyl) (*33, 35, 36*), such generation of transient ketyl radical should be possible if there is an appropriate base near the C-3 hydroxy group of DOIA. Thus, although the participation of a disulfide bond or other electron sink mechanism cannot be excluded, at this point, it is reasonable to presume that further oxidation of the DOIA radical proceeds via a transient ketyl radical through proton-coupled electron transfer (PCET), which is known to be a critical mechanism for oxidations and reductions of radical species in several other biological systems such as galactose oxidase and P450 enzymes (*12, 13, 37, 38*). Furthermore, it is noteworthy that a ketyl

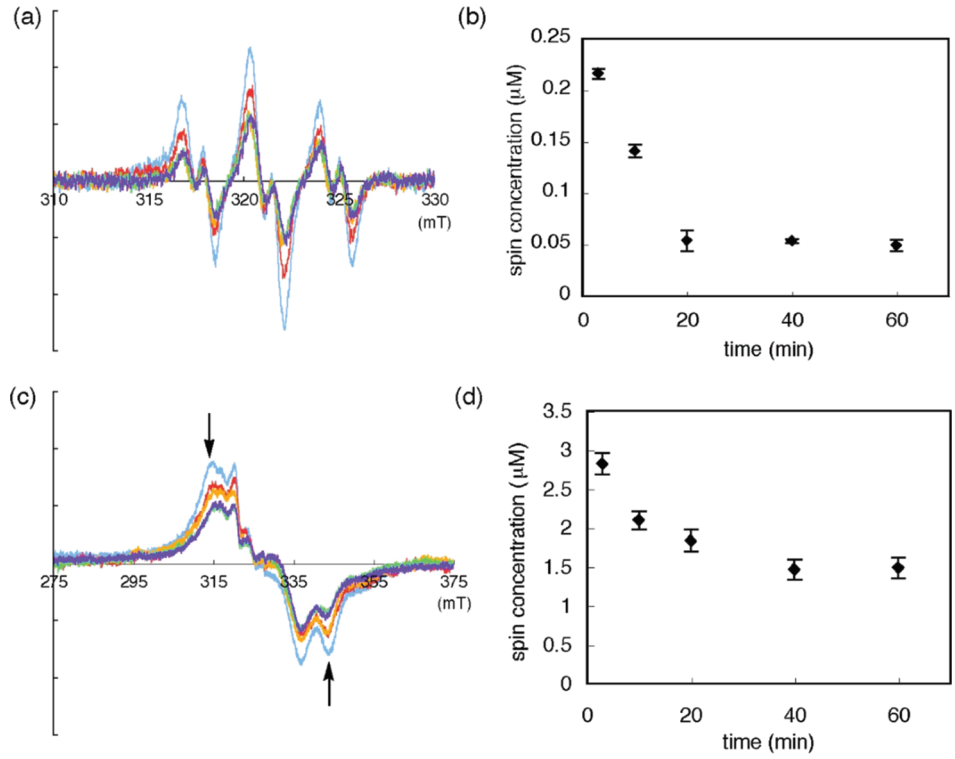


FIGURE 8: Time course of the EPR signals. Enzyme reaction conditions were identical to those described in the legend of Figure 1. (a) Time course of the EPR signal of the DOIA radical recorded at 50 K. Recording conditions were identical to those described in the legend of Figure 1: (blue line) 3 min, (red line) 10 min, (orange line) 20 min, (green line) 40 min, and (purple line) 60 min. (b) Time course of the spin concentration of the DOIA radical, calculated by comparison of a double integral of each signal with a standard $Cu(II)SO_4$. (c) Time course of the EPR signal of the 4Fe−4S cluster. EPR spectra were recorded at 10 K, with a microwave power of 1 mW to prevent saturation. Other recording conditions were identical to those described in the legend of Figure 3: (blue line) 3 min, (red line) 10 min, (orange line) 20 min, (green line) 40 min, and (purple line) 60 min. (d) Time course of the spin concentration of the rhombic signal estimated from the comparison of the peak-to-peak intensity of the $g = 1.89$ and 2.04 features with that of the signal shown in Figure 3a whose concentration was determined to be 2.1 $\mu$M as described in the text.

radical was recently identified as an intermediate in a reaction catalyzed by 2-hydroxy-4-methylpentanoyl-CoA dehydratase (*39*).

As for the reaction catalyzed by radical SAM enzymes, observations of radical intermediates are quite limited. Lysine-2,3-aminomutase is the only radical SAM enzyme so far for which the organic radical intermediate had been characterized in the presteady state and in the steady state of the reaction (*40–43*). Substrate-derived organic radical species were also reported for the reaction of coproporphyrinogen III oxidase, HemN (*44*). In the HemN reaction, organic radical species were observed only when the subsequent electron transfer reaction was interrupted by the omission of an outside electron acceptor. This study is now the second example of a radical intermediate observed in the steady state and presteady state of a reaction catalyzed by a radical SAM enzyme.

In this series of EPR measurements, no organic radical that can be assigned as the 5′-deoxyadenosyl radical was observed, while the signal for the putative BtrN−SAM−DOIA complex and the DOIA radical intermediate were observed. Even a reaction with 2-deoxy-*scyllo*-[3-$^2$H]inosamine that should slow the hydrogen atom abstraction did not result in the accumulation of the 5′-deoxyadenosyl radical (data not shown). Since the SAM cleavage was shown to be reversible in this reaction (*14*), these results indicate that the subsequent hydrogen atom abstraction and/or the reverse reaction to regenerate SAM is fast, which makes the 5′-deoxyadenosyl radical exist only transiently. The transient nature of the 5′-deoxyadenosyl radical is likely to be a common feature for radical SAM enzymes, since such radical species are observed only when an allylic analogue of SAM is used (*45, 46*).

The EPR spectrum of the 4Fe−4S cluster during the reaction was also recorded, and the signals for a free BtrN, a BtrN−SAM complex, and a rhombic signal presumably derived from the BtrN−SAM−DOIA ternary complex were observed (Figure 3). The assignment of the rhombic signal as the BtrN−SAM−DOIA ternary complex was accomplished by the comparison of the signal with those of other BtrN−substrate and BtrN−product complexes. The time course of the EPR signal revealed the presteady state accumulation of the rhombic signal as well as that of the DOIA radical intermediate, which indicates that the rhombic signal is derived from an intermediate before the rate-determining step, ketone formation, and thus further supports the assignment of the rhombic signal to the BtrN−SAM−DOIA ternary complex. The signal for the BtrN−DOIA complex was not observed during the reaction, which is consistent with the previously proposed kinetic mechanism that SAM binds first to free BtrN and then DOIA binds to the BtrN−SAM complex. The time course of the EPR spectra showed that the signals of the DOIA radical and 4Fe−4S clusters were all decreased in the presteady state without the formation of any new signals. Since the BtrN−product complexes show no characteristic feature in EPR (Figure 5), the decrease in the magnitude of the EPR signal of the Fe−S

cluster indicates the formation of BtrN−product complexes. The invisibilities of these complexes are further discussed below.

The significant differences in EPR signals among free BtrN, the BtrN−SAM complex, and the BtrN−SAM−DOIA complex are quite intriguing. As for other radical SAM enzymes, SAM has been shown to coordinate directly to the vacant site of the 4Fe−4S cluster according to X-ray crystallographic analyses and ENDOR experiments (*30, 31, 47–51*). In addition, significant EPR signal changes have been observed upon binding of SAM for pyruvate formate lyase activase and class III ribonucleotide reductase activase (*51–53*). BtrN also exhibited a change in EPR signal upon SAM binding, indicating a direct coordination of SAM to the 4Fe−4S cluster. Perturbation of the EPR signal by addition of DOIA to the free BtrN solution (Figure 3c) and the change from axial signal of the BtrN−SAM complex to the rhombic signal of the BtrN−SAM−DOIA ternary complex (Figure 7) suggest that DOIA also affects the electronic state of the 4Fe−4S cluster directly or through a protein conformational changing. Such an interaction may trigger the reductive cleavage of SAM and generation of the DOIA radical intermediate (*34, 54*).

Although most of the EPR signals observed in this study are reasonably interpreted as described above, the decrease in the EPR signal intensity upon binding of the products remains unresolved. Since UV−vis absorption spectra did not change (Figure 6), a change in the redox state of the cluster is unlikely. One possible explanation is a change in the spin state of the cluster from $S = {}^1/_2$ to $S = {}^3/_2$, ${}^5/_2$, or ${}^9/_2$. EPR signals of such high-spin state 4Fe−4S clusters should be broadened and might have escaped detection at the low concentrations used in our experiments. Experiments that aim to characterize this EPR silent Fe−S cluster are ongoing.

In conclusion, we have successfully observed the DOIA radical intermediate by EPR measurements, which strongly suggests the radical mechanism of BtrN. Furthermore, EPR signals for free BtrN, the BtrN−SAM complex, and a rhombic signal presumably derived from the BtrN−SAM−DOIA ternary complex were also observed during the reaction. Significant changes in signal features among those complexes suggest electronic interactions of both substrates with the 4Fe−4S cluster. Our observations should aid in the understanding of the whole catalytic cycle of BtrN and other radical SAM dehydrogenases.

## SUPPORTING INFORMATION AVAILABLE

Activity assay of EDTA-treated BtrN, EPR power saturation experiments, EPR spectra of prolonged incubation of the BtrN reaction mixture, HPLC charts, and NMR spectra. This material is available free of charge via the Internet at http://pubs.acs.org.

## REFERENCES


1. Pauly, T. A., Ekstrom, J. L., Beebe, D. A., Chrunyk, B., Cunningham, D., Griffor, M., Kamath, A., Lee, S. E., Madura, R., McGuire, D., Subashi, T., Wasilko, D., Watts, P., Mylari, B. L., Oates, P. J., Adams, P. D., and Rath, V. L. (2003) X-ray crystallographic and kinetic studies of human sorbitol dehydrogenase. *Structure 11*, 1071–1085.
2. Ishikawa, K., Higashi, N., Nakamura, T., Matsuura, T., and Nakagawa, A. (2007) The first crystal structure of L-threonine dehydrogenase. *J. Mol. Biol. 366*, 857–867.
3. Jornvall, H., Persson, B., Krook, M., Atrian, S., Gonzalez-Duarte, R., Jeffery, J., and Ghosh, D. (1992) Short-chain dehydrogenases reductases (SDR). *Biochemistry 34*, 6003–6013.
4. Benach, J., Atrian, S., GonzaÁlez-Duarte, R., and Ladenstein, R. (1998) The refined crystal structure of *Drosophila lebanonensis* alcohol dehydrogenase at 1.9 Å resolution. *J. Mol. Biol. 282*, 383–399.
5. Cavener, D. R. (1992) GMC oxidoreductases. A newly defined family of homologous proteins with diverse catalytic activities. *J. Mol. Biol. 223*, 811–814.
6. Fan, F., and Gadda, G. (2005) On the catalytic mechanism of choline oxidase. *J. Am. Chem. Soc. 127*, 2067–2074.
7. Zheng, Y. J., Xia, Z., Chen, Z., Mathews, F. S., and Bruice, T. C. (2001) Catalytic mechanism of quinoprotein methanol dehydrogenase: A theoretical and X-ray crystallographic investigation. *Proc. Natl. Acad. Sci. U.S.A. 98*, 432–434.
8. Xia, Z. X., Dai, W. W., Xiong, J. P., Hao, Z. P., Davidson, V. L., White, S., and Mathews, F. S. (1992) The three-dimensional structures of methanol dehydrogenase from two methylotrophic bacteria at 2.6 Å resolution. *J. Biol. Chem. 267*, 22289–22297.
9. Meunier, B., de Visser, S. P., and Shaik, S. (2004) Mechanism of oxidation reactions catalyzed by cytochrome P450 enzymes. *Chem. Rev. 104*, 3947–3980.
10. Oh, N. Y., Suh, Y., Park, M. J., Seo, M. S., Kim, J., and Nam, W. (2005) Mechanistic insight into alcohol oxidation by high-valent iron(IV) oxo complexes of heme and nonheme ligands. *Angew. Chem., Int. Ed. 44*, 4235–4239.
11. Vaz, A. D., and Coon, M. J. (1994) On the mechanism of action of cytochrome P450: Evaluation of hydrogen abstraction in oxygen-dependent alcohol oxidation. *Biochemistry 33*, 6442–6449.
12. Stubbe, J., and van der Donk, W. A. (1998) Protein Radicals in Enzyme Catalysis. *Chem. Rev. 98*, 705–762.
13. Whittaker, J. W. (2003) Free radical catalysis by galactose oxidase. *Chem. Rev. 103*, 2347–2363.
14. Yokoyama, K., Numakura, M., Kudo, F., Ohmori, D., and Eguchi, T. (2007) Characterization and mechanistic study of a radical SAM dehydrogenase in the biosynthesis of butirosin. *J. Am. Chem. Soc. 129*, 15147–15155.
15. Fang, Q., Peng, J., and Dierks, T. (2004) Post-translational formylglycine modification of bacterial sulfatases by the radical S-adenosylmethionine protein AtsB. *J. Biol. Chem. 279*, 14570–14578.
16. Benjdia, A., Leprince, J., Guillot, A., Vaudry, H., Rabot, S., and Berteau, O. (2007) Anaerobic sulfatase-maturating enzymes: Radical SAM enzymes able to catalyze in vitro sulfatase post-translational modification. *J. Am. Chem. Soc. 129*, 3462–3463.
17. Fish, W. W. (1988) Rapid colorimetric micromethod for the quantitation of complexed iron in biological samples. *Methods Enzymol. 158*, 357–364.
18. Hernandez, H. L., Pierrel, F., Elleingand, E., Garcia-Serres, R., Huynh, B. H., Johnson, M. K., Fontecave, M., and Atta, M. (2007) MiaB, a bifunctional radical-S-adenosylmethionine enzyme involved in the thiolation and methylation of tRNA, contains two essential [4Fe-4S] clusters. *Biochemistry 46*, 5140–5147.
19. Layer, G., Grage, K., Teschner, T., Schunemann, V., Breckau, D., Masoumi, A., Jahn, M., Heathcote, P., Trautwein, A. X., and Jahn, D. (2005) Radical S-adenosylmethionine enzyme coproporphyrinogen III oxidase HemN: Functional features of the [4Fe-4S] cluster and the two bound S-adenosyl-L-methionines. *J. Biol. Chem. 280*, 29038–29046.
20. Broderick, J. B., Duderstadt, R. E., Fernandez, D. C., Wojtuszewski, K., Henshaw, T. F., and Johnson, M. K. (1997) Pyruvate formate-lyase activating enzyme is an iron-sulfur protein. *J. Am. Chem. Soc. 119*, 7396–7397.
21. Kudo, F., Hosomi, Y., Tamegai, H., and Kakinuma, K. (1999) Purification and characterization of 2-deoxy-scyllo-inosose synthase derived from *Bacillus circulans*. A crucial carbocyclization enzyme in the biosynthesis of 2-deoxystreptamine-containing aminoglycoside antibiotics. *J. Antibiot. 52*, 81–88.
22. Tamegai, H., Nango, E., Kuwahara, M., Yamamoto, H., Ota, Y., Kuriki, H., Eguchi, T., and Kakinuma, K. (2002) Identification of L-glutamine: 2-Deoxy-scyllo-inosose aminotransferase required for the biosynthesis of butirosin in *Bacillus circulans*. *J. Antibiot. 55*, 707–714.
23. Kuwata, T., and Ito, K. (1980) in *Introduction to Electron Spin Resonance*, Nankodo, Tokyo.

24. Behshad, E., Ruzicka, F. J., Mansoorabadi, S. O., Chen, D., Reed, G. H., and Frey, P. A. (2006) Enantiomeric free radicals and enzymatic control of stereochemistry in a radical mechanism: The case of lysine 2,3-aminomutases. *Biochemistry 45*, 12639–12646.
25. Jen, C. K., Foner, S. N., Cochran, E. L., and Bowers, V. A. (1958) Electron spin resonance of atomic and molecular free radicals trapped at liquid helium temperature. *Phys. Rev. 112*, 1169–1182.
26. Fessenden, R. W., and Schuler, R. H. (1963) Electron spin resonance studies of transient alkyl radicals. *J. Chem. Phys. 39*, 2147–2195.
27. Yokoyama, K., Kudo, F., Kuwahara, M., Inomata, K., Tamegai, H., Eguchi, T., and Kakinuma, K. (2005) Stereochemical recognition of doubly functional aminotransferase in 2-deoxystreptamine biosynthesis. *J. Am. Chem. Soc. 127*, 5869–5874.
28. Huang, F., Li, Y., Yu, J., and Spencer, J. B. (2002) Biosynthesis of aminoglycoside antibiotics: Cloning, expression and characterisation of an aminotransferase involved in the pathway to 2-deoxystreptamine. *Chem. Commun.,* 2860–2861.
29. Yamauchi, N., and Kakinuma, K. (1992) Biochemical studies on 2-deoxy-scyllo-inosose, an earliest intermediate in the biosynthesis of 2-deoxystreptamine. I. Chemical synthesis of 2-deoxy-scyllo-inosose and [2,2-$^2H_2$]-2-deoxy-scyllo-inosose. *J. Antibiot. 45*, 756–766.
30. Hanzelmann, P., and Schindelin, H. (2004) Crystal structure of the S-adenosylmethionine-dependent enzyme MoaA and its implications for molybdenum cofactor deficiency in humans. *Proc. Natl. Acad. Sci. U.S.A. 101*, 12870–12875.
31. Berkovitch, F., Nicolet, Y., Wan, J. T., Jarrett, J. T., and Drennan, C. L. (2004) Crystal structure of biotin synthase, an *S*-adenosylmethionine-dependent radical enzyme. *Science 303*, 76–79.
32. Grove, T. L., Lee, K. H., St Clair, J., Krebs, C., and Booker, S. J. (2008) In vitro characterization of AtsB, a radical SAM formylglycine-generating enzyme that contains three [4Fe-4S] clusters. *Biochemistry 47*, 7523–7538.
33. Rao, P. S., and Hayon, E. (1976) Correlation between ionization constants of organic free radicals and electrochemical properties of parent compounds. *Anal. Chem. 48*, 564–568.
34. Hinckley, G. T., and Frey, P. A. (2006) Cofactor dependence of reduction potentials for $[4Fe\text{-}4S]^{2+/1+}$ in lysine 2,3-aminomutase. *Biochemistry 45*, 3219–3225.
35. Silva, C. O., da Silva, E. C., and Nascimento, M. A. C. (2000) Ab Initio calculations of absolute $pK_a$ values in aqueous solution. II. Aliphatic alcohols, thiols, and halogenated carboxylic acids. *J. Phys. Chem. A 104*, 2402–2409.
36. Stewart, R. (1985) in *The Proton: Applications to Organic Chemistry*, Vol. 46, Academic Press, New York.
37. Reece, S. Y., Hodgkiss, J. M., Stubbe, J., and Nocera, D. G. (2006) Proton-coupled electron transfer: The mechanistic underpinning for radical transport and catalysis in biology. *Philos. Trans. R. Soc. London, Ser. B 361*, 1351–1364.
38. Stubbe, J., Nocera, D. G., Yee, C. S., and Chang, M. C. (2003) Radical initiation in the class I ribonucleotide reductase: Long-range proton-coupled electron transfer? *Chem. Rev. 103*, 2167–2201.
39. Kim, J., Darley, D. J., Buckel, W., and Pierik, A. J. (2008) An allylic ketyl radical intermediate in clostridial amino-acid fermentation. *Nature 452*, 239–242.
40. Ballinger, M. D., Frey, P. A., and Reed, G. H. (1992) Structure of a substrate radical intermediate in the reaction of lysine 2,3-aminomutase. *Biochemistry 31*, 10782–10789.
41. Ballinger, M. D., Frey, P. A., Reed, G. H., and LoBrutto, R. (1995) Pulsed electron paramagnetic resonance studies of the lysine 2,3-aminomutase substrate radical: Evidence for participation of pyridoxal 5′-phosphate in a radical rearrangement. *Biochemistry 34*, 10086–10093.
42. Wu, W., Lieder, K. W., Reed, G. H., and Frey, P. A. (1995) Observation of a second substrate radical intermediate in the reaction of lysine 2,3-aminomutase: A radical centered on the $\beta$-carbon of the alternative substrate, 4-thia-L-lysine. *Biochemistry 34*, 10532–10537.
43. Chang, C. H., Ballinger, M. D., Reed, G. H., and Frey, P. A. (1996) Lysine 2,3-aminomutase: Rapid mix-freeze-quench electron paramagnetic resonance studies establishing the kinetic competence of a substrate-based radical intermediate. *Biochemistry 35*, 11081–11084.
44. Layer, G., Pierik, A. J., Trost, M., Rigby, S. E., Leech, H. K., Grage, K., Breckau, D., Astner, I., Jansch, L., Heathcote, P., Warren, M. J., Heinz, D. W., and Jahn, D. (2006) The substrate radical of *Escherichia coli* oxygen-independent coproporphyrinogen III oxidase HemN. *J. Biol. Chem. 281*, 15727–15734.
45. Magnusson, O. T., Reed, G. H., and Frey, P. A. (1999) Spectroscopic evidence for the participation of an allylic analogue of the 5′-deoxyadenosyl radical in the reaction of lysine 2,3-aminomutase. *J. Am. Chem. Soc. 121*, 9764–9765.
46. Magnusson, O. T., Reed, G. H., and Frey, P. A. (2001) Characterization of an allylic analogue of the 5′-deoxyadenosyl radical: An intermediate in the reaction of lysine 2,3-aminomutase. *Biochemistry 40*, 7773–7782.
47. Lepore, B. W., Ruzicka, F. J., Frey, P. A., and Ringe, D. (2005) The X-ray crystal structure of lysine-2,3-aminomutase from *Clostridium subterminale*. *Proc. Natl. Acad. Sci. U.S.A. 102*, 13819–13824.
48. Layer, G., Moser, J., Heinz, D. W., Jahn, D., and Schubert, W. D. (2003) Crystal structure of coproporphyrinogen III oxidase reveals cofactor geometry of radical SAM enzymes. *EMBO J. 22*, 6214–6224.
49. Chen, D., Walsby, C., Hoffman, B. M., and Frey, P. A. (2003) Coordination and mechanism of reversible cleavage of S-adenosylmethionine by the [4Fe-4S] center in lysine 2,3-aminomutase. *J. Am. Chem. Soc. 125*, 11788–11789.
50. Walsby, C. J., Ortillo, D., Broderick, W. E., Broderick, J. B., and Hoffman, B. M. (2002) An anchoring role for FeS clusters: Chelation of the amino acid moiety of S-adenosylmethionine to the unique iron site of the [4Fe-4S] cluster of pyruvate formate-lyase activating enzyme. *J. Am. Chem. Soc. 124*, 11270–11271.
51. Walsby, C. J., Hong, W., Broderick, W. E., Cheek, J., Ortillo, D., Broderick, J. B., and Hoffman, B. M. (2002) Electron-nuclear double resonance spectroscopic evidence that S-adenosylmethionine binds in contact with the catalytically active $[4Fe\text{-}4S]^+$ cluster of pyruvate formate-lyase activating enzyme. *J. Am. Chem. Soc. 124*, 3143–3151.
52. Padovani, D., Thomas, F., Trautwein, A. X., Mulliez, E., and Fontecave, M. (2001) Activation of class III ribonucleotide reductase from *E. coli*. The electron transfer from the iron-sulfur center to *S*-adenosylmethionine. *Biochemistry 40*, 6713–6719.
53. Liu, A., and Graslund, A. (2000) Electron paramagnetic resonance evidence for a novel interconversion of $[3Fe\text{-}4S]^+$ and $[4Fe\text{-}4S]^+$ clusters with endogenous iron and sulfide in anaerobic ribonucleotide reductase activase in vitro. *J. Biol. Chem. 275*, 12367–12373.
54. Wang, S. C., and Frey, P. A. (2007) Binding energy in the one-electron reductive cleavage of S-adenosylmethionine in lysine 2,3-aminomutase, a radical SAM enzyme. *Biochemistry 46*, 12889–12895.


BI800509X